

Solid-state NMR study of locations and dynamics of interlayer cations and water in kanemite

Shigenobu Hayashi

National Institute of Materials and Chemical Research, 1-1 Higashi, Tsukuba, Ibaraki 305, Japan

The locations and dynamics of interlayer sodium (Na) cations and water in kanemite have been studied by means of solid-state ^1H , ^{29}Si and ^{23}Na NMR. In addition to one-dimensional (1D) spectra, ^1H - ^{29}Si two-dimensional (2D) cross-polarization (CP) correlation, ^{23}Na 2D nutation and ^{23}Na 2D triple-quantum spectra were also measured. Hydroxy groups have a large ^1H chemical shift (15 ppm from tetramethylsilane), forming strong hydrogen bonds of the $\text{Si}-\text{O}-\text{H}\cdots\text{O}^- - \text{Si}$ type between the layers. When the amount of water is large, the water molecules are mobile in the interlayer space. With a decrease in the water content, the motion of the water is restricted. There is only one type of Si site in undried kanemite. The decrease in the water content affects the layer structure, which is indicated by a new ^{29}Si peak. The site of Na^+ species has an isotropic chemical shift of 2.9 ppm from 1 mol dm^{-3} NaCl aqueous solution, a quadrupole coupling constant of 2.05 MHz and an asymmetry factor of 0.63. The Na^+ species do not rotate isotropically, but have a fixed orientation. Water molecules do not coordinate to the Na ions directly.

Kanemite, of ideal formulation $\text{NaHSi}_2\text{O}_5 \cdot 3\text{H}_2\text{O}$,¹ is a layered material consisting of single layers of SiO_4 tetrahedra.² Kanemite as well as other alkali-metal silicate minerals have potential uses as catalyst supports and novel absorbents. Kanemite can be used as the starting compound for the synthesis of the mesoporous material FSM-16.^{3,4} Benek and Lagacy have studied the inner crystalline reactivity of kanemite in detail.¹ However, the crystal structure of kanemite has not, as yet, been established. The structure of kanemite is likely to be similar to that of KHSi_2O_5 whose structure is known.⁵

Kanemite contains sodium ions and water molecules in the interlayer space. The sodium ions are easily exchanged.¹ A portion of the water molecules are desorbed by drying over P_2O_5 or by treatment with ethylene glycol, resulting in the reduction of the basal spacing.¹ Consequently, water molecules are an important element in the structure of kanemite.

Solid-state NMR is a useful technique to study local structures and dynamics of interlayer species as well as the structure of the SiO_4 network in layered alkali-metal silicates.⁶⁻¹² The layers are connected by strong hydrogen bonding, which is supported by a large frequency shift of the ^1H signal of the hydroxy groups.⁸⁻¹¹ Almond *et al.*^{9,11} and Apperley *et al.*¹⁰ have concluded that the hydroxy groups are the source of cross polarization (CP) in magadiite, octosilicate and kanemite. Almond *et al.* considered that the rigid nature of the hydroxy group makes the efficiency of the cross polarization high, whereas water molecules are too mobile for efficient CP.¹¹ These workers used dried samples, and thus, strictly speaking, the structures might be different from those of the undried samples.

In the present work, the behaviour of the interlayer species in kanemite has been studied by solid-state NMR spectroscopy for undried and mildly dried samples. The interlayer species as well as the SiO_4 network might be sensitive to water molecules. Mild drying treatment affected the amount and the location of water molecules, and subsequently influenced the mobilities of sodium ions and water molecules, as well as the structure of the SiO_4 network.

Experimental

Materials

Kanemite was synthesized according to the procedures described in the literature.^{1,3,4} Sodium silicate solution with

an $\text{SiO}_2/\text{Na}_2\text{O}$ ratio of 2 was obtained from Wako Pure Chemical Industries, Ltd. (Japan). The solution was heated in an electric furnace. The temperature was raised to 700°C in 0.5 h, kept at that value for 5.5 h, and then cooled to room temperature over 6 h. The resulting material was dispersed in water and the solid phase separated by centrifugation and filtration. Finally it was dried at room temperature (*ca.* 20°C).

The powder X-ray diffraction pattern of the as-synthesized sample was measured on a Rigaku RAX-01 Geiger Flex diffractometer. The pattern was in accord with those obtained by Yanagisawa *et al.*³ and Inagaki *et al.*⁴ The basal spacing was 1.027 nm.

The amount of water was controlled by mild heating in air. In addition to the as-synthesized sample (designated H20), two samples were prepared by heating at 40 and 80°C for about 3 h, samples H40 and H80.

TG-DTA

Thermogravimetric (TG) and differential thermal analyses (DTA) were performed on a Rigaku Thermoflex TG8110 to determine the amount of residual water. The sample temperature was raised at a rate of $10^\circ\text{C min}^{-1}$ up to 500°C in air.

NMR measurements

NMR measurements were carried out on Bruker MSL400, ASX400 and ASX200 spectrometers with static magnetic field strengths of 9.4, 9.4 and 4.7 T, respectively. Unless otherwise stated, the same measurements were made at the two different magnetic fields.

^1H one-dimensional (1D) spectra were measured using the single pulse sequence under fast magic angle spinning (MAS) conditions. The recycle time was 1.0 s. Larmor frequencies were 400.13 and 200.13 MHz.

^{29}Si 1D MAS spectra were traced using the single pulse sequence with and without ^1H decoupling (denoted HD and SP, respectively) and the cross-polarization (CP) sequence. Larmor frequencies were 79.49 and 39.76 MHz. Two-dimensional (2D) ^1H - ^{29}Si cross-polarization spectra were measured on a Bruker ASX200 instrument using the pulse sequence proposed by Vega.¹³

^{23}Na 1D spectra were measured using the single pulse sequence with and without ^1H decoupling and the cross-polarization sequence for both spinning and static samples. Larmor frequencies were 105.84 and 52.94 MHz. 2D nutation

spectra were also measured for static samples at the two magnetic fields. 2D triple-quantum (TQ) spectra were measured under MAS conditions with the ASX400 spectrometer. The three-pulse shifted-echo sequence proposed by Massiot *et al.*¹⁴ was used.

Spectra were presented with the following signals being 0 ppm; neat tetramethylsilane for ¹H and ²⁹Si and 1 mol dm⁻³ NaCl aqueous solution for ²³Na. The higher frequency side of the spectrum with respect to the standard signal was expressed as positive.

Results and Discussion

TG-DTA

Fig. 1 shows TG curves for the samples H20, H40 and H80. There are four steps in the dehydration process: step A up to 47°C, step B from 47 to 85°C, step C from 85 to 136°C and step D above 136°C. The mass decrease finishes at about 400°C. The boundary temperatures for the three samples agree within the experimental errors. Table 1 summarizes the TG data. The amount of water is expressed by *x* in the form NaHSi₂O₅·*x*H₂O; note that the amount of hydroxy groups is evaluated in the form of H₂O.

According to Beneke and Lagaly,¹ there are two types of water in the interlayer space: one type forms an interlamellar monolayer of water molecules, while the other is trapped within vacancies of the folded SiO₃OH hexagonal rings. The amounts of the two types of water molecules are *x*=1.8 and 1.0, respectively. Kanemite transforms above 700°C into tridymite, which retains some water in the structure; 92% of the total water content is desorbed by 300°C.

Each step in TG can not be assigned to one particular

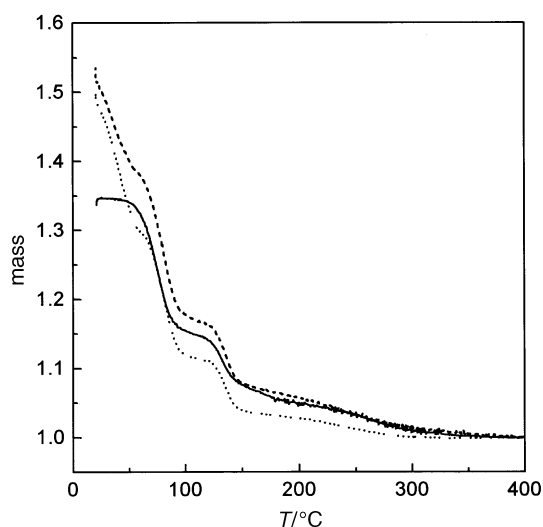


Fig. 1 TG curves for the samples H20 (···), H40 (---) and H80 (—). The temperature was increased at a rate of 10°C min⁻¹. Masses are normalized by that of the dehydrated sample.

Table 1 Summary of TG results

sample	<i>x</i> ^a in each step (T/°C)				total <i>x</i>
	A	B	C	D	
H20	1.8 (21–47)	1.6 (47–85)	0.7 (85–136)	0.4 (136–300)	4.5
H40	1.3 (21–46)	1.9 (46–85)	0.9 (85–138)	0.7 (138–400)	4.8
H80	0 (21–39)	1.7 (39–81)	0.7 (81–134)	0.7 (134–380)	3.2

^aAccording to the formula NaHSi₂O₅·*x*H₂O.

species exclusively. In addition to the interlayer water molecules, there are water molecules adsorbed on the external surface or in the intercrystalline region and hydroxy groups as the source of the evolved water. The surface water is released in step A, and some of the hydroxy groups are released in step D. Interlamellar water may be released in both steps A and B while water within the hexagonal rings might be released in both steps C and D.

After thermal treatment at 40°C, the total amount of water is not changed. Surface water probably migrates into the structure, since the water released in steps B, C and D is increased by the treatment. Thermal treatment at 80°C leads to the disappearance of surface water and also some interlamellar water.

¹H NMR

Fig. 2 shows ¹H MAS NMR spectra measured at 400.13 MHz. Two isotropic peaks are observed at 15 and 5 ppm, ascribed to hydroxy groups and water molecules.

The total amount of water and hydroxy groups was measured by TG, although experimental errors of *ca.* 10% are estimated. According to NMR the fractions of protons existing as hydroxy groups are 1/11, 1/11 and 1/5 for samples H20, H40 and H80, respectively, corresponding to *x*=0.4, 0.4 and 0.6. These values agree, within experimental error, to the ideal value (*x*=0.5). Step D in the TG curves for samples H40 and H80 is considered to involve release of water within the hexagonal rings, since *x*>0.5. In total, *x*=4.1, 4.4 and 2.5 for samples H20, H40 and H80, respectively, compared with 3 for an ideal composition. The excess water is presumed to be adsorbed on the external surface.

The full width at half maximum of the 15 ppm peak is *ca.* 6 ppm (2.4 kHz), and is unaffected by heat treatment. On the other hand, the linewidth of the 5 ppm peak increases upon heat treatment, being 1.0 ppm (0.40 kHz), 2 ppm (0.8 kHz) and 10 ppm (4.0 kHz) for the three samples, respectively.

Spectra were also measured at 200.13 MHz. The linewidth of the 15 ppm peak was 12 ppm (2.4 kHz) for all three samples. This linewidth is in accord with the value at the high magnetic field in Hz, suggesting that the linewidth is of dipolar origin. The linewidths of the 5 ppm peak are 1.4 ppm (0.28 kHz),

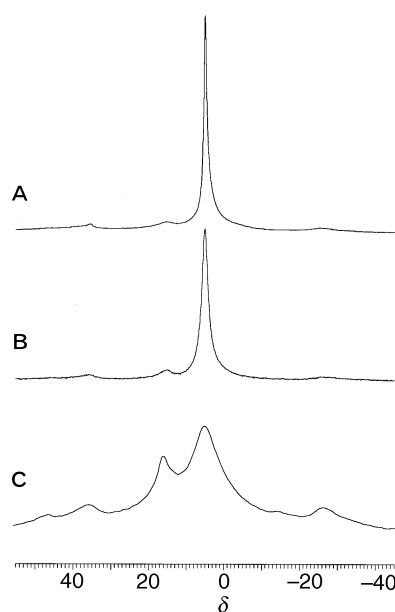


Fig. 2 ¹H MAS NMR spectra, measured at 400.13 MHz, for (A) H20, (B) H40 and (C) H80. Sample spinning rate, 12.00 kHz. Peaks outside the range of 30 to -10 ppm are spinning sidebands.

4 ppm (0.8 kHz) and 19 ppm (3.8 kHz) for the samples H20, H40 and H80, respectively; the last two samples have a linewidth (Hz) independent of the field. Dipolar interaction is considered to be the dominant mechanism in the line broadening and motion of the water is restricted, especially in the sample H80. In contrast, the linewidth of the sample H20 is dependent on the field strength. Inhomogeneous broadening is accompanied by homogeneous broadening, suggesting that the water molecules are mobile.

^{29}Si NMR

Fig. 3 shows ^{29}Si MAS NMR spectra. Sample H20 shows a signal at -97.3 ppm, as shown in Fig. 3A, which is assigned to Q^3 (Q^n refers to SiO_4 tetrahedra with n bridging oxygens). A small hump at -109 ppm is ascribed to Q^4 species in impurity phases such as amorphous silica. The SP and HD spectra have the same linewidth of 1.5 ppm, demonstrating that there is a negligible contribution of dipolar interactions with ^1H . The efficiency of cross polarization from ^1H to ^{29}Si is very low.

Sample H40 shows almost the same spectrum as sample H20. The linewidth in the SP spectrum (1.8 ppm) is a little broader than in the HD and CP spectra (1.5 ppm), indicating a small contribution of ^1H dipolar interactions; however, the CP efficiency is still low.

The sample H80 shows two signals at -97.1 and -95.3 ppm (Fig. 3B and C), also assigned to Q^3 silicon. The -97.1 ppm peak lies essentially at the same position as in samples H20 and H40, whereas the -95.3 ppm peak is new. The higher frequency shift implies a smaller mean $\text{Si}-\text{O}-\text{Si}$ angle,^{15,16} suggesting shrinkage of the SiO_4 network. The linewidths are broader in the SP spectra than in the CP and HD spectra indicating that the CP efficiency is much higher for sample H80 than for samples H20 and H40. These facts are consistent with the ^1H NMR results that the water motion is restricted in sample H80.

The ^{29}Si chemical shift value reported by Yanagisawa *et al.* is -97.2 ppm,³ which is in accord with our results for samples H20 and H40. On the other hand, the value reported by Apperley *et al.*, -95 ppm,¹⁰ upon drying their sample at 60°C , is in accord with the higher frequency peak of sample H80. The discrepancy between the literature values is thus a consequence of the difference in the water contents in the samples.

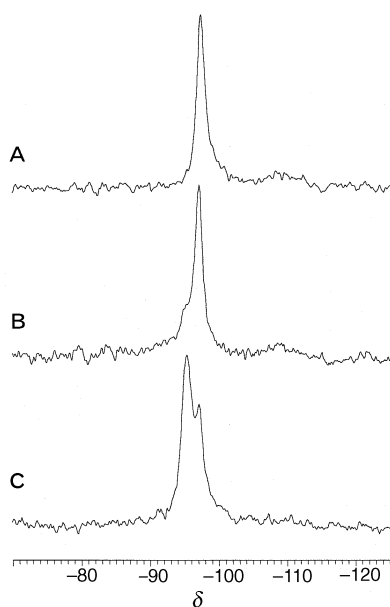


Fig. 3 ^{29}Si MAS NMR spectra measured at 79.49 MHz. (A) HD for sample H20 and (B) HD and (C) CP for sample H80. Sample spinning rates, (A) 3.50 kHz, (B,C) 3.00 kHz. The contact time for CP was 5 ms.

The relative intensities of the two peaks for sample H80 are different in the HD and CP spectra, as shown in Fig. 3B and C, and Fig. 4 shows contact time dependences of the signal intensities. The cross relaxation times T_{SiH} are 1.3 and 0.35 ms for the -95.3 and -97.1 ppm peaks, respectively. In the case of silica gel, $T_{\text{SiH}}=2.3$ and 2.9 ms for $\text{Si}(\text{OSi})_2(\text{OH})_2$ and $\text{Si}(\text{OSi})_3(\text{OH})$, respectively.¹⁷ The measured values for sample H80 are thus lower than those of silica gel. Water entrapped within the hexagonal rings and a part of the interlamellar water are considered to play a role in the cross polarization. The contribution of water is larger in the -97.1 ppm peak than in the -95.3 ppm peak, which can be explained by the loss of water in the vicinity of Si atoms corresponding to the -95.3 ppm peak. The ^1H spin-lattice relaxation time in the rotating frame, $T_{1\rho}(^1\text{H})$, is 3.5 ms for both peaks. The two species are cross-polarized from the same energy reservoir formed by the ^1H dipolar network, suggesting that the two species are fairly close to each other.

^1H - ^{29}Si 2D CP correlation spectra have been measured for samples H20 and H80 at 39.76 MHz and at a spinning rate of 10.00 kHz (spectra not shown) and correlation between the ^{29}Si signals and water is observed. Cross polarization from hydrogen-bonded protons to Si has been observed in dried magadiite, kanemite and octosilicate.⁹⁻¹¹ In those cases, the ^1H signals were sharp and clearly resolved, indicating that spin diffusion between the hydroxy groups and water is suppressed. In the present case, however, spin diffusion between hydroxy groups and water may operate.

^{23}Na NMR

Na ions are located in the interlayer space and generally, assumed to be coordinated by water molecules in layered silicates. Almond *et al.*¹² have reported that there is one Na site in kanemite. They derived an isotropic chemical shift (δ_{iso}) of 5 and a quadrupole coupling constant ($\chi = e^2Qq/h$) of 2 MHz from the field dependence of the second-order quadrupole shift, assuming that the asymmetry factor of the quadrupole interaction (η_Q) is zero. In the present work, the nature of the Na site is investigated in detail.

Fig. 5 shows HD MAS NMR spectra of samples H40 and H80, measured at two magnetic fields. The field dependence of the lineshape demonstrates that it is determined predominantly by a second-order quadrupole interaction. However, the lineshapes indicate more than one component. To analyse the lineshape further, we also measured spectra for static samples, as shown in Fig. 6. The sample H20 shows the same lineshapes as sample H40.

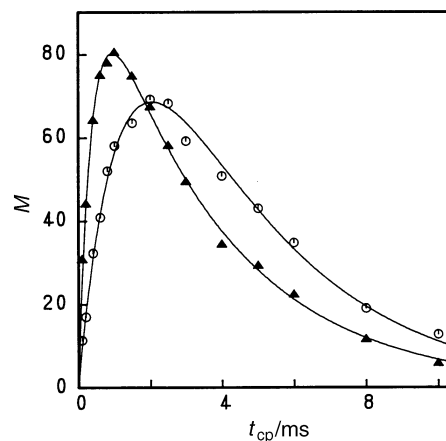


Fig. 4 Contact time dependences of ^{29}Si signal intensities M at -95.3 (\circ) and -97.1 ppm (\blacktriangle) in CP MAS NMR spectra of sample H80, measured at 79.49 MHz. Curves show least-square fits using a theoretical formula.

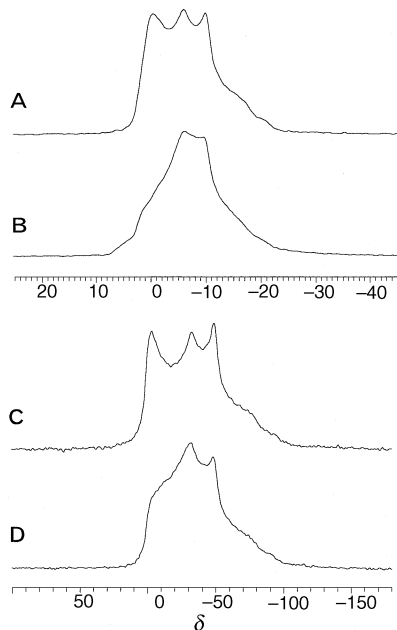


Fig. 5 ^{23}Na HD MAS NMR spectra, measured at 105.84 MHz for (A) sample H40 and (B) sample H80, and at 52.94 MHz for (C) sample H40 and (D) sample H80. Sample spinning rate, 12.00 kHz.

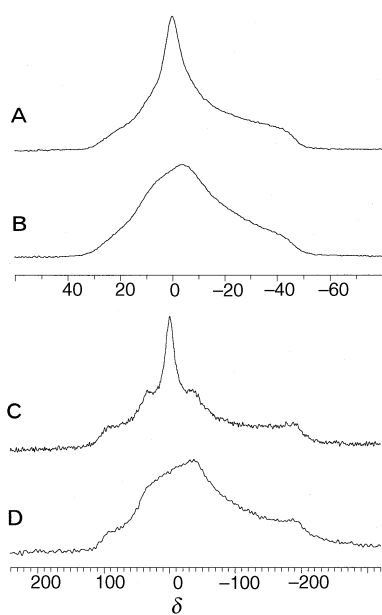


Fig. 6 ^{23}Na HD static NMR spectra, measured at 105.84 MHz for (A) sample H40 and (B) sample H80, and at 52.94 MHz for (C) sample H40 and (D) sample H80

When ^1H decoupling is removed, line broadening occurs for sample H80, no broadening is observed for sample H20, while sample H40 shows a slight broadening. These results are explained by the mobility of the water molecules in the vicinity of the Na ions. CP is inefficient for sample H40, while a weak distorted signal is observed for sample H80. This result is also explained by the mobility of the water. For kenyaite, CP can distinguish two Na sites: one bound in the mineral lattice without neighbouring protons, while the other resides between layers.¹⁸ CP is effective for the latter, since the Na ion is in close proximity to the interstitial water molecules. On the other hand, in dried magadiite, CP takes place from the hydrogen-bonding hydroxy groups rather than water molecules.¹² Kanemite has a larger quadrupole interaction than

kenyaite and magadiite, resulting in low CP efficiency even for the sample H80.

To differentiate the Na sites, we have attempted to measure 2D NMR spectra. Fig. 7 shows 2D nutation NMR spectra of samples H40 and H80; the spectrum of H20 is essentially the same as that of sample H40. The spectra of H20 and H40 show two components with very different quadrupole interactions. While the amplitude of the ^{23}Na pulse used in the experiment is *ca.* 60 kHz the quadrupole coupling constants of the two components are much smaller and much larger than 60 kHz, respectively. In contrast, sample H80 shows only one component with a quadrupole coupling constant much larger than 60 kHz.

To check whether the signal with the large quadrupole interaction consists of only one component, we have measured 2D TQ MAS NMR spectra. Fig. 8 shows the spectra for samples H20 and H80. One component is observed for sample H20, whereas at least two components are seen for sample H80. In the sample H20, the component with the small quadrupole interaction does not produce a signal in the 2D TQ MAS spectrum, since triple quantum coherence is generated by the perturbation on the spin levels caused by quadrupole coupling.

In conclusion, samples H20 and H40 consist of two components with small and large quadrupole interactions. On the other hand, sample H80 consists of two components with large quadrupole interactions.

Using the above information, we simulated the 1D spectra, and the results are partly shown in Fig. 9 and 10 for samples H40 and H80 measured at 52.94 MHz under MAS; other 1D spectra measured under different conditions are similar. Sample H20 gives very similar results to H40. Component I dominates in all three samples. This component has $\delta_{\text{iso}} = 2.9$ ppm, $\chi = 2.05$ MHz and $\eta_Q = 0.63$, and is independent of the water content. The fraction of component I is 85–90% of the total Na. The residual components do not have the characteristic lineshape expected for a second-order quadrupole interaction. The χ and η_Q values are considered to have wide distributions. Therefore, the residual components are assumed to have a

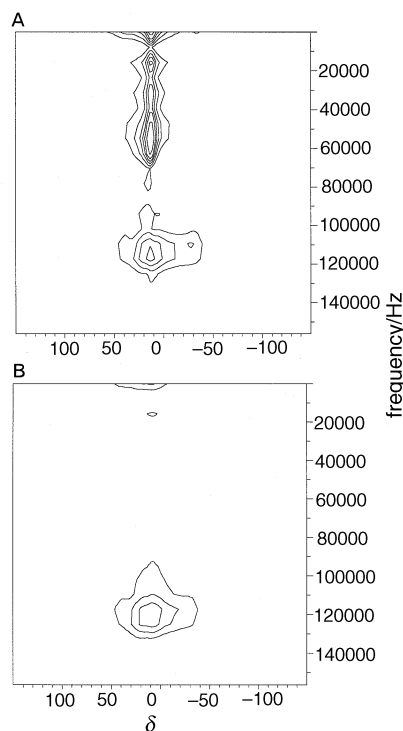


Fig. 7 ^{23}Na 2D nutation NMR spectra, measured at 105.84 MHz for static samples. (A) Sample H40 and (B) sample H80.

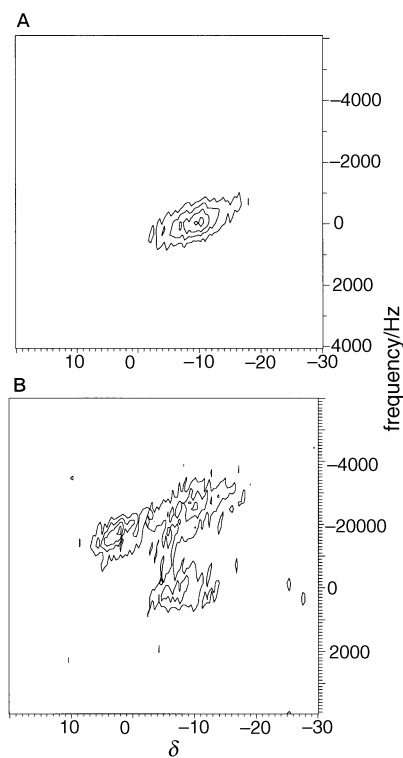


Fig. 8 ^{23}Na 2D TQ MAS NMR spectra, measured at 105.84 MHz. (A) Sample H20 and (B) sample H80. Sample spinning rate, 10.00 kHz.

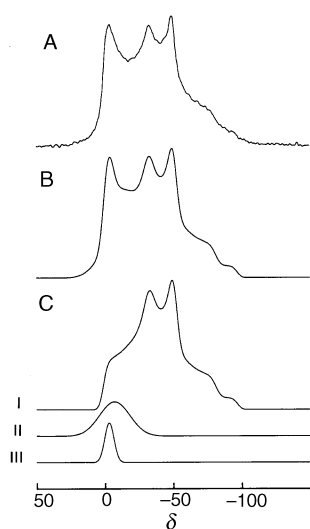


Fig. 9 (A) ^{23}Na HD MAS NMR spectrum of sample H40, measured at 52.94 MHz, (B) its simulated spectrum and (C) component spectra used in the simulation

Gaussian lineshape for simplicity. Two additional components, II and III, are necessary to simulate the lineshape.

Locations and dynamics of sodium ions and water

The structure of kanemite is likely to be similar to that of KHSi_2O_5 .¹⁰ Fig. 11 shows the structure of kanemite schematically, including a defect region.

Hydroxy groups have a large ^1H chemical shift (15 ppm), forming strong hydrogen bonds between the layers with the bonds considered to be of the $\text{Si}-\text{O}-\text{H}\cdots\text{O}^- - \text{Si}$ type. Water molecules can be classified into three types: external surface water, interlamellar water ($\text{H}_2\text{O}_{\text{IL}}$) and hole water ($\text{H}_2\text{O}_{\text{Hole}}$). The external surface water is mobile and desorbs easily upon thermal treatment. The interlamellar water desorb sub-

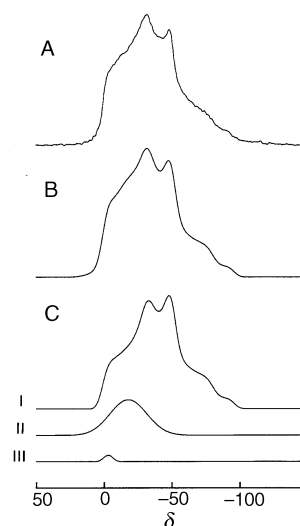


Fig. 10 (A) ^{23}Na HD MAS NMR spectrum of sample H80, measured at 52.94 MHz, (B) its simulated spectrum and (C) component spectra used in the simulation

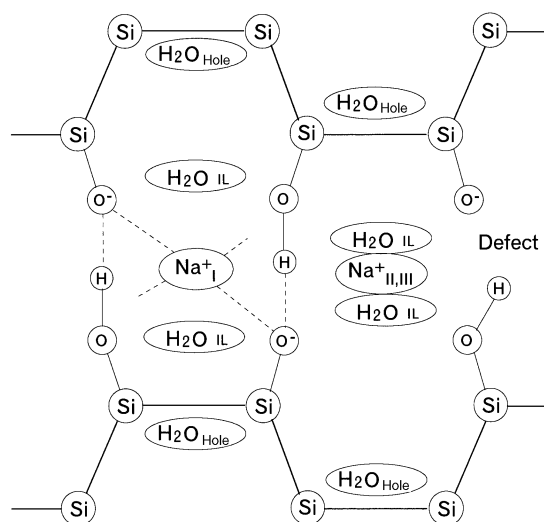


Fig. 11 Schematic structure of kanemite, including a defect region

sequently, while the hole water within the hexagonal rings is unevolved until after the desorption of the interlamellar water. The maximum amounts of the interlamellar and hole water are *ca.* $x=2$ and 1, respectively (for $\text{NaHSi}_2\text{O}_5 \cdot x\text{H}_2\text{O}$). When the amount of the interlamellar water is *ca.* 2, the interlamellar water is mobile in the interlayer space. With decreasing water content, the interlayer distance decreases, and subsequently the motion of the interlamellar water is restricted, which is supported by the appearance of the dipolar interactions between ^1H spins. The hole water is trapped within the holes of the folded SiO_3OH hexagonal rings, and their motion is even more restricted than that of the interlamellar water.

There is only one Si site in undried kanemite, as confirmed by ^{29}Si NMR spectroscopy. Formally, half of the Si sites are $\text{Si}-\text{OH}$, and the other half are $\text{Si}-\text{O}^- \text{Na}^+$. The strong hydrogen bond $\text{Si}-\text{O}-\text{H}\cdots\text{O}^- - \text{Si}$ might decrease any shift difference, if present, between the above two forms. A decrease in interlamellar water affects the layer structure, producing a higher frequency shift of the ^{29}Si signal; such interlayer water is important in retention of the structure. Water molecules are located in the vicinity of Si atoms, as confirmed from the cross polarization efficiency.

The dominant Na^+ species included in the samples have

$\delta_{\text{iso}} = 2.9$ ppm, $\chi = 2.05$ MHz and $\eta_Q = 0.63$. These values are not changed upon mild heat treatment. The Na^+ species do not rotate isotropically, but have a fixed orientation. In a lattice of kanemite, Na^+ species are considered to be coordinated by several oxygen atoms forming part of the SiO_4 network, but water molecules do not coordinate to the Na^+ species directly. If mobile water were coordinated to Na^+ , then the Na^+ species should be mobile. If mobile water molecules spent part of their time coordinated to Na^+ , the quadrupole interaction should be perturbed by the water whereas the experimental results demonstrate that the water content does not influence the Na^+ site. If water molecules were rigidly coordinated to Na^+ a dipolar interaction with ^1H should be observed clearly irrespective of the water content. The dipolar interaction between ^{23}Na and ^1H is observed experimentally only when the motion of the water is restricted. This suggests that water molecules are located in the vicinity of the Na^+ species. Almond *et al.* speculated from the chemical shift and the quadrupole coupling constant that the Na^+ species are coordinated by five oxygen atoms in either the SiO_4 network or water molecules.¹² However, because of the lack of a sufficient database, the coordination number cannot be determined.

A part of the Na^+ species show a change in magnitude of quadrupole interaction upon heat treatment. Before the treatment, the quadrupole coupling constant is $\ll 60$ kHz. These Na^+ species are considered to be hydrated in the undried sample, *i.e.*, water molecules are coordinated directly to Na^+ species. These hydrated species can rotate isotropically and may be located in defect regions of the layer structure, the external surface, or amorphous impurity phase regions. With the decrease in the total water content, such Na^+ species are dehydrated, and their motions are restricted.

In zeolite cages, Na ions are hydrated in the ambient atmosphere and the apparent chemical shift and the linewidth in the ^{23}Na MAS NMR spectra of NaY zeolite are -12 ppm and 1.2 kHz (23 ppm) at 52.80 MHz.¹⁹ Upon heat treatment the Na ions are dehydrated although the zeolite cage is retained, and hydration can reoccur. The Na ions in the zeolite cage are similar to the minor species in kanemite. Exchangeable Na ions in the interlayer space of tetrasilicic sodium fluormica (TSM) show $\delta_{\text{iso}} = 6$ ppm and $\chi = 2.24$ MHz.²⁰ The quadrupole coupling constant is comparable to the value of kanemite. Upon addition of water, these Na ions become hydrated and mobile. The interlayer distance of TSM increases substantially upon hydration.

Conclusions

The following conclusions are derived from the ^1H , ^{29}Si and ^{23}Na NMR results.

(i) Hydroxy groups have a large ^1H chemical shift (15 ppm), forming strong $\text{Si}-\text{O}-\text{H}\cdots\text{O}^- - \text{Si}$ type hydrogen bonds

between the layers. At high levels of hydration, the interlayer water is mobile. With a decrease in the water content, the interlayer distance decreases, and subsequently the motion of the water is restricted.

(ii) There is only one Si site in undried kanemite, as confirmed by ^{29}Si NMR spectroscopy. The decrease in the interlayer water affects the layer structure, which is indicated by the appearance of a new peak in the ^{29}Si spectrum.

(iii) The Na site in the kanemite lattice has $\delta_{\text{iso}} = 2.9$ ppm, $\chi = 2.05$ MHz and $\eta_Q = 0.63$. These values are unaltered upon mild heat treatment. The Na^+ species do not rotate isotropically, but have a fixed orientation. Water molecules are not coordinated to these Na^+ species directly.

The author is grateful to Mr. M. Satozawa and Prof. K. Kunimori of University of Tsukuba for the synthesis of kanemite.

References

- 1 K. Beneke and G. Lagaly, *Am. Mineral.*, 1977, **62**, 763.
- 2 M. T. Le Bihan, A. Kalt and R. Wey, *Bull. Soc. Fr. Miner. Cristallogr., Sect. B*, 1968, **24**, 13.
- 3 T. Yanagisawa, T. Shimizu, K. Kuroda and C. Kato, *Bull. Chem. Soc. Jpn.*, 1990, **63**, 988.
- 4 S. Inagaki, Y. Fukushima and K. Kuroda, *J. Chem. Soc., Chem. Commun.*, 1993, 680.
- 5 M. T. Le Bihan, A. Kalt and R. Wey, *Bull. Soc. Fr. Miner. Cristallogr.*, 1971, **94**, 15.
- 6 T. J. Pinnavaia, I. D. Johnson and M. Lipsicas, *J. Solid State Chem.*, 1986, **63**, 118.
- 7 J. M. Rajo, E. Ruiz-Hitzky and J. Sanz, *Inorg. Chem.*, 1988, **27**, 2785.
- 8 Z. Q. Deng, J. F. Lambert and J. J. Fripiat, *Chem. Mater.*, 1989, **1**, 375.
- 9 G. G. Almond, R. K. Harris and P. Graham, *J. Chem. Soc., Chem. Commun.*, 1994, 851.
- 10 D. C. Apperley, M. J. Hudson, M. T. J. Keene and J. A. Knowles, *J. Mater. Chem.*, 1995, **5**, 577.
- 11 G. G. Almond, R. K. Harris and K. R. Franklin, *Solid State Nucl. Magn. Reson.*, 1996, **6**, 31.
- 12 G. G. Almond, R. K. Harris, K. R. Franklin and P. Graham, *J. Mater. Chem.*, 1996, **6**, 843.
- 13 A. J. Vega, *J. Am. Chem. Soc.*, 1988, **110**, 1049.
- 14 D. Massiot, B. Touzo, D. Trumeau, J. P. Coutures, J. Virlet, P. Florian and P. J. Grandinetti, *Solid State Nuc. Magn. Reson.*, 1996, **6**, 73.
- 15 J. M. Thomas, J. Klinowski, S. Ramdas, B. K. Hunter and D. T. B. Tennakoon, *Chem. Phys. Lett.*, 1983, **102**, 158.
- 16 S. Ramdas and J. Klinowski, *Nature (London)*, 1984, **308**, 521.
- 17 G. E. Maciel and D. W. Sindorf, *J. Am. Chem. Soc.*, 1980, **102**, 7607.
- 18 R. K. Harris and G. J. Nesbitt, *J. Magn. Reson.*, 1988, **78**, 245.
- 19 S. Hayashi, K. Hayamizu and O. Yamamoto, *Bull. Chem. Soc. Jpn.*, 1987, **60**, 105.
- 20 M. Soma, A. Tanaka, H. Seyama, S. Hayashi and K. Hayamizu, *Clay Sci.*, 1990, **8**, 1.

Paper 6/07528B; Received 5th November, 1996